Journal of Molecular Catalysis A: Chemical 424 (2016) 220–231

Contents lists available at ScienceDirect

Journal of Molecular Catalysis A: Chemical

journal homepage: www.elsevier.com/locate/molcata

Vanadium(III)–catalyzed copolymerization of ethylene with norbornene: Microstructure at tetrad level and reactivity ratios

Giuseppe Leone[a], Ivana Pierro[a,b], Giorgia Zanchin[a,c], Alessandra Forni[d], Fabio Bertini[a], Arnaldo Rapallo[a,*], Giovanni Ricci[a,*]

[a] CNR-Istituto per lo Studio delle Macromolecole (ISMAC), via E. Bassini 15, I-20133 Milano, Italy
[b] Dipartimento di Scienze Chimiche, Università degli Studi di Napoli Federico II, Complesso Monte S. Angelo, Via Cintia, I-80126 Napoli, Italy
[c] Dipartimento di Chimica, Università degli Studi di Milano, via C. Golgi 19, I-20133 Milano, Italy
[d] CNR-Istituto di Scienze e Tecnologie Molecolari (ISTM), via C. Golgi 19, I-20133 Milano, Italy

ARTICLE INFO

Article history:
Received 4 August 2016
Received in revised form 30 August 2016
Accepted 2 September 2016
Available online 4 September 2016

Keywords:
Cyclic olefin copolymers
V(III) catalysis
Stereospecific polymerization
Microstructure
Catalytic mechanisms
Reactivity ratios
NMR

ABSTRACT

Vanadium(III) complex bearing $PMePh_2$ ligand has been synthesized, fully-characterized and investigated for homo- and co-polymerization of ethylene with norbornene, in combination with aluminum compounds, i.e., methylaluminoxane (MAO) and Et_2AlCl. The results are carefully compared with those obtained with $VCl_3(THF)_3$ and VCl_3 in the presence and absence of ethyltrichloroacetate (ETA), and free phosphine. $VCl_3(PMePh_2)_2$ was likely activated through a dissociative mechanism where the dissociation of the labile phosphine ligand was the first and possibly the rate-determining step. The activity of $VCl_3(THF)_3$ was slightly higher than that of $VCl_3(PMePh_2)_2$ likely due to a different competition of re-insertion rate of dissociated ligand compared to the insertion/coordination of (co)monomers. Copolymers obtained at low norbornene feedstock concentration from $VCl_3(THF)_3$, showed greater non-uniformity in terms of composition distribution with respect to those from $VCl_3(PMePh_2)_2$ because of a more pronounced compositional drift in the semi-batch polymerization process. This strongly affects the copolymer's thermal properties, the copolymers from $VCl_3(PMePh_2)_2$ exhibiting higher T_gs. The effect of $PMePh_2$ and THF ligand on reactions responsible for chain growth termination, affecting the copolymers molecular weight, is discussed. Control over the norbornene incorporation and molecular weight of the resultant copolymers proved to be possible by changing the polymerization temperature, and ETA loading.

In addition, *ad-hoc.* experiments, designed to ensure the uniformity of the catalytic copolymerization process even in the presence of the observed relevant (and unavoidable) compositional drift were performed, and copolymers microstructure and catalytic mechanisms were thoroughly investigated. Due to the peculiar features of the catalytic systems, these studies could be performed only after appropriate modifications to well established methods were developed. As a by-product of these investigations, general and original computational methods are proposed, whose applicability goes beyond the cases treated here.

1. Introduction

Cyclic olefins copolymers (COCs) have gained attention owing to their unique properties which make them attractive as high-tech engineering plastics. The most versatile and interesting COCs are those of ethylene with norbornene. These copolymers are a promising class of thermoplastics, ranging from highly crystalline solids to thermoplastic elastomers, whose properties depend on the norbornene content and copolymer microstructure [1]. A significant breakthrough in this area was achieved when Kaminsky et al. discovered that the C_2-symmetric metallocenes, in combination with MAO, catalyzed the copolymerization of ethylene with cyclic olefins [2]. Hence, Group 4 metal complexes, including half–sandwich [3], and Cp–free [4], late transition Ni-[5], and Pd-[6] complexes, and rare–earth metal complexes have been developed [7].

In contrast, Group 5 metal complexes remain less explored in spite of the fact that vanadium catalysts are largely employed for the fabrication of (*i*) synthetic rubber and elastomers [8], (*ii*) high molecular weight poly(ethylene) [9], (*iii*) syndiotactic

* Corresponding authors.
E-mail addresses: arnaldo.rapallo@ismac.cnr.it (A. Rapallo), giovanni.ricci@ismac.cnr.it (G. Ricci).

http://dx.doi.org/10.1016/j.molcata.2016.09.002
1381-1169/

poly(propylene) [10], and (*iv*) COCs commercialized as APEL® by Mitsui Chemicals, Inc [11]. Facile reduction to inactive V(II) species [12], intrinsical instability of V—C bond [13], paramagnetic oxidation states, and unfavourable olefin association/dissociation [14], are some drawback encountered by vanadium catalysts. Nonetheless, some vanadium complexes, through an appropriate ligand modification, and in combination with an aluminum alkyl and ETA reoxidant, gave results comparable with those of the more established Group 4 metals, in terms of activity and cyclic olefin incorporation [12]. Most of these catalyst systems are based on V(V) complexes with arylimido-aryloxo [15], amine pyridine(s) phenolate [16], and tetradentate amine trihydroxy ligands [17], and V(III) complexes supported by multidentate ligands having, in different combination, N and O hard donor atoms [12].

V(III) complexes bearing amine bis(phenolate) ligands copolymerize ethylene with norbornene to random copolymers, exhibiting low activity [18]. Use of mono(β-enaminoketonato) N∧O ligands improved the overall productivity and mainly alternating copolymers were obtained [19]. Later, the introduction of a pendant L heteroatom in the bidentate N∧O Schiff base ligand gave V(III) complexes which exhibited the highest activity in ethylene/norbornene copolymerization with L = phosphorus donor. Indeed, N∧O ligands with pendant phosphine group, in which the phosphorous atom is bound to the nitrogen through a rigid phenylene bridge, help to strengthen the phospine coordination, stabilizing the V(III) species [20]. As a matter of fact, the ligand denticity plays a fundamental role in influencing the stability of V(III) complexes. However, with respect to the starting $VCl_3(THF)_3$, the modifications introduced in the ligand did not have always a significant effect on the activities, composition and copolymers microstructure. Highest activities and norbornene incorporations were attained with $VCl_3(THF)_3$ despite the labile nature of THF ligand.

In recent years, there has also been renewed interest concerning trivalent phosphine ligands in transition metal (d-block) coordination and organometallic chemistry [21]. Phosphine-containing complexes were recently found to promote hydroboration of alkenes [22], hydrogenation of carboxylic acids to alcohols [23], hydroxycarbonylation [24], sodium bicarbonate hydrogenation [25], and cyclic olefin (co)polymerization [26]. However, only few examples of V(III)–phosphine complexes are reported so far and none of these has ever been used as catalyst for the stereospecific olefins (co)polymerization [27].

Herein, we report the synthesis, crystal structure and ethylene homo- and co-polymerization with norbornene behaviour of $VCl_3(PMePh_2)_2$. Excellent activities and a tendency to give atactic, alternating copolymers were observed. The results are carefully compared with those obtained with $VCl_3(THF)_3$ and VCl_3 in the presence and absence of ETA and free $PMePh_2$. The effect of $PMePh_2$ and THF labile ligand on the activity, the reactions responsible for chain growth termination, the copolymers microstructure and properties is discussed.

In addition, thorough mechanistic studies were performed after appropriate adaptation of theoretical methods of analysis to account for the specificity of the V(III) complexes under investigation. The study of binary copolymers microstructure from ^{13}C NMR and of copolymerization mechanisms according to the theory of homogeneous Markov chains, is a long-standing topic within the polymer chemists community [28]. These studies range from the analysis of the bare content of comonomers to the characterization of the microstructure in terms of diads, triads, tetrads, and above. Concerning the determination of the experimental microstructure, it is essential to work with high quality NMR spectra, and to accurately evaluate the peaks areas. This is very often done by direct integration of the spectrum, but in cases of strong peaks overlap it may be difficult to separate the contributions coming from different peaks. Deconvolving the NMR spectrum can provide a more robust route to the calculation of the areas. Given the diversity of fields where deconvolution is a required step, various free or commercial general purpose software exist for performing deconvolution in one, two, and three dimensions. Anyway, a straightforward procedure is proposed in this work, based on the Richardson-Lucy algorithm [29], which proved to be particularly well suited in the case of NMR spectra, since it naturally enforces the positivity constraint, and it is very robust with respect to the noise corrupting the signal.

Concerning the study of catalytic mechanism, the copolymerizations must be performed in such a way that the homogeneity prerequisite of the Markov chain is granted, at least approximately. In homogeneous Markov chains the conditional probabilities of monomers insertion given a certain last inserted sequence are constants. On the contrary, in the experiments, these probabilities are functions of the conversion, and change during the polymerization, which leads to non-homogeneous conditions. The applicability of the theoretical tool of homogeneous Markov chain requires that the polymerization reactions are stopped at low conversion (<5%) to stay as close as possible within a homogeneity regime.

V(III) based catalysts studied in this work displayed an impressive activity, and norbornene conversions beyond 50% were reached already in experiments less than one minute long, thus breaking the applicability of the standard theoretical tools to study the catalytic mechanisms. This fact may explain why no detailed mechanistic studies are reported in the literature for many types of vanadium complexes, displaying analogous behaviour [12,18–20]. Herein, a Monte Carlo based computational original approach is developed to model the copolymerization process, which fully takes into account the non-homogeneity conditions proper to the high conversion regimes. By means of this tool, both the order of the catalytic mechanism and the reactivity ratios can be evaluated at high conversions. The proposed method is robust and allows to work with very detailed experimental microstructural information, when available: from the bare content of the comonomers up to the undecads. Since it relies on very general principles, its use is not limited to the investigated catalysts, and any case of binary copolymerization can be treated without modifications of the algorithms.

2. Experimental section

2.1. General procedures and materials

Manipulations of air- and/or moisture-sensitive materials were carried out under an inert atmosphere using a dual vacuum/nitrogen line and standard Schlenk-line techniques. THF (Aldrich, ≥99.9% pure) was refluxed over Na/benzophenone alloy for 8 h and then distilled and stored over molecular sieves. Toluene (Fluka, >99.5% pure) was refluxed over Na for 8 h and then distilled and stored over molecular sieves. Pentane (Aldrich, >99% pure) was refluxed over Na/K alloy for 8 h and then distilled and stored over molecular sieves. ETA (Aldrich, 97%) was stirred over CaH_2 for about 4 h and then distilled trap-to-trap. Diethylaluminium chloride (Et_2AlCl, Aldrich), MAO (10 wt.% solution in toluene, Aldrich), $PMePh_2$ and $VCl_3(THF)_3$ (Aldrich) were used as received. Norbornene (Aldrich, 99% pure) was stirred over molten potassium at 80 °C under nitrogen for 4 h and then distilled. A stock solution was prepared by dissolving 50 g of freshly distilled norbornene in 86.2 mL of toluene. Ethylene was purified by passage over columns of $CaCl_2$, molecular sieves, and BTS catalysts. Deuterated solvent for NMR measurements ($C_2D_2Cl_4$) (Aldrich, >99.5% atom D) was used as received.

2.2. Synthesis of $VCl_3(PMePh_2)_2$

$VCl_3(PMePh_2)_2$ complex was synthesized using the method of Bultitude et al. [27c] with some changes. $PMePh_2$ (2.19 g, 11 mmol) was added to a suspension of $VCl_3(THF)_3$ (1.02 g, 2.73 mmol, P/V = 4:1) in 15 mL of toluene at room temperature, giving immediate formation of a red-purple suspension containing an orange solid. The mixture was left under stirring overnight. The solution was filtered and then concentrated to half of its volume. 50 mL of pentane was subsequently added, dropwise, at room temperature, over which time a red-purple precipitate was formed. The suspension was filtered and the solvent then removed under vacuum. The residual red-purple solid was washed twice with 30 mL of pentane and the resultant precipitate filtered and dried under vacuum to give $VCl_3(PMePh_2)_2$ as a red-purple powder (Yield, 90%).

FTIR: 3053 (w), 1588 (w), 1483 (mw), 1435 (m), 1296 (w), 1130 (s), 1096 (m), 1026 (w), 994 (m), 885 (s), 780 (mw) 741 (vs), 690 (vs), 505 (s), 477 (m).

The solid obtained was then extracted continuously with boiling pentane. Crystals of $VCl_3(PMePh_2)_2$ were formed directly on the bottom of the Schlenk tube during the extraction, and further crops of crystals were obtained by cooling the supernatant pentane solution at −30 °C.

2.3. X-ray structure determination of $VCl_3(PMePh_2)_2$

The intensity data were collected on a Bruker Smart Apex CCD area detector using graphite-monochromated Mo Kα radiation (λ = 0.71073 Å). Data reduction was made using SAINT programs; absorption corrections based on multiscan were obtained by SADABS [30]. The structures were solved by SHELXS-97 [31], and refined on F^2 by full-matrix least-squares using SHELXL-14 [32]. All the non-hydrogen atoms were refined anisotropically, hydrogen atoms were included as 'riding' and not refined. The isotropic thermal parameters of H atoms were fixed at 1.2 (1.5 for methyl groups) times the equivalent thermal parameter of the atoms to which they are bonded. Crystal data and results of the refinement: air-sensitive red tablet 0.37 × 0.37 × 0.15 mm, M_w = 557.70, triclinic, space group P-1, a = 11.8722(7) Å, b = 13.1864(7) Å, c = 17.6804(10) Å, α = 74.0516(8)°, β = 88.8531(9)°, γ = 88.1796(9)°, V = 2659.8(3) Å^3, Z = 4, T = 130(2) K, μ = 0.807 mm^{-1}. 57731 measured reflections, 18106 independent reflections, 13934 reflections with $I > 2\sigma(I)$, $2.40 < 2\theta < 64.67°$, R_{int} = 0.0358. Refinement on 18106 reflections, 581 parameters. Final R = 0.0483, wR = 0.1225 for data with $F^2 > 2\sigma(F^2)$, S = 1.028, $(\Delta/\sigma)_{max}$ = 0.001, $\Delta\rho_{max}$ = 1.595, $\Delta\rho_{min}$ = −1.622 eÅ^{-3}. CCDC 1478267 contains the supplementary crystallographic data for this paper. These data can be obtained free of charge from The Cambridge Crystallographic Data Centre via www.ccdc.cam.ac.uk/data_request/cif.

2.4. Molecular modelling calculations on $VCl_3(PMePh_2)_2$

Geometry optimization of the isolated, gas phase $VCl_3(PMePh_2)_2$ molecule was performed by the Gaussian09 program package [33], using the M06 functional and the 6–311g(d) basis set, starting from the X-ray structure of molecule A (Fig. 1). Optimization of the hypothetical 'eclipsed' conformation, whose starting geometry has been obtained by rotating one $PMePh_2$ group by 120° around the P—V bond axis, was also performed. According to previous magnetic measurements, [27a] both conformations were modeled in their triplet state through the unrestricted formalism. The triplet states were found to be more stable than the corresponding singlet states by 35 kcal/mol.

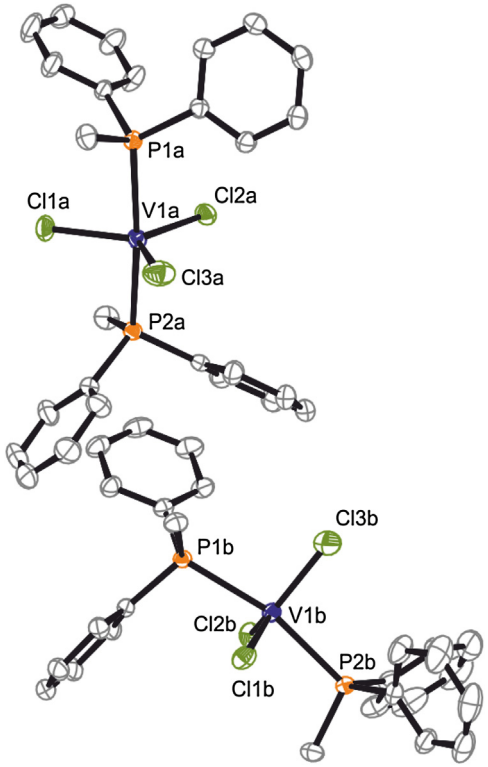

Fig. 1. Molecular structure of $VCl_3(PMePh_2)_2$ [molecule A (top), molecule B (bottom)] with thermal ellipsoids drawn at 50% probability level. Hydrogen atoms omitted for clarity.

2.5. General copolymerization procedure

Polymerizations were carried out in a 25 mL round-bottomed Schlenk flask. Prior to starting polymerization, the reactor was heated to 110 °C under vacuum for 1 h and backfilled with nitrogen. The reactor was charged at room temperature with toluene, norbornene, ETA and the aluminum coumpound in that order. After thermal equilibration at the desired temperature, the solution was degassed and ethylene was added until saturation. Polymerization was started by adding a toluene solution (2 mg mL^{-1}) of vanadium complex via syringe under continuous flow of ethylene. Polymerizations were stopped with methanol containing a small amount of hydrochloric acid; the precipitated polymers were collected by filtration, repeatedly washed with fresh methanol and finally dried in vacuum at room temperature to constant weight.

2.6. Characterization

Attenuated total reflectance (ATR)-Fourier transform infrared spectroscopy (FTIR) spectra were recorded at room temperature in the 4000–600 cm^{-1} range with a resolution of 4 cm^{-1} using a Perkin Elmer Spectrum Two spectrometer. NMR spectra were recorded on a Bruker NMR advance 400 Spectrometer operating at 400 MHz (^{1}H) and 100.58 MHz (^{13}C) working in the PFT mode at 103 °C. ^{13}C experiments were performed with 10 mm probe in $C_2D_2Cl_4$ and referred to hexamethyldisiloxane (HMDS), as internal standard. The relaxation delay was 16 s. Differential scanning calorimetry (DSC) scans were carried out on a Perkin-Elmer Pyris 1 instrument equipped with a liquid subambient device under helium atmosphere. The sample, typically 5 mg, was placed in a sealed aluminum pan, and the measurement was carried out from −80 to 150 °C using heating and cooling rate of 20 °C min^{-1}. The molecular weight average (M_w) and the molecular weight distribution (M_w/M_n) were obtained by a high temperature Waters GPCV2000

Table 1
Polymerization of ethylene catalyzed by $VCl_3(PMePh_2)_2$, $VCl_3(THF)_3$, and VCl_3.[a]

entry	catalyst system	yield (g)	activity[b]	M_w[c] ($\times 10^{-3}$)	M_w/M_n[c]
1	$VCl_3(PMePh_2)_2/Et_2AlCl$	0.13	156	308.1	4.2
2	$VCl_3(PMePh_2)_2/Et_2AlCl/ETA$	0.50	1200	22.4	4.3
3	$VCl_3(PMePh_2)_2/MAO$	traces			
4	$VCl_3(PMePh_2)_2/MAO/ETA$	0.16	384	900.0	25
5	$VCl_3(THF)_3/Et_2AlCl$	0.13	156	178.4	2.2
6	$VCl_3(THF)_3/Et_2AlCl/ETA$	0.57	1368	19.4	5.6
7	$VCl_3(THF)_3/MAO$	traces			
8	$VCl_3(THF)_3/MAO/ETA$	0.31	744	367.0	12.5
9	VCl_3/Et_2AlCl	inactive			
10	$VCl_3/Et_2AlCl/ETA$	traces			

[a] Polymerization conditions: ethylene pressure, 1.01 bar; total volume, 25 mL (toluene); V-complex, 5 μmol; Al/V = 2000; ETA/V = 300; temperature, 22 °C; time, 5 min.
[b] Activity in $kg_{pol}\ mol_V^{-1}\ h^{-1}$.
[c] Determined by SEC.

size exclusion chromatography (SEC) system equipped with a refractometer detector. The experimental conditions consisted of three PL Gel Olexis columns, *ortho*-dichlorobenzene (DCB) as the mobile phase, 0.8 mL min^{-1} flow rate, and 145 °C temperature. The calibration of the SEC system was constructed using eighteen narrow M_w/M_n poly(styrene) standards with molar weights ranging from 162 to 5.6×10^6 g mol^{-1}. For SEC analysis, about 12 mg of polymer was dissolved in 5 mL of DCB with 0.05% of BHT as antioxidant.

2.7. Calculation of tetrad distribution and reactivity ratios

A computational program to perform the deconvolution of the NMR spectra has been developed in OpenMP Fortran 90 language, based on the Richardson-Lucy algorithm [29]. A Monte Carlo algorithm implemented in the same language has also been developed for determining the reactivity ratios at high conversion regimes. Both tools has been used to study the microstructures of two copolymers at the tetrad level, and to elucidate the catalytic mechanism of the V(III) based catalysts studied in this work.

3. Results and discussion

3.1. Synthesis, structure and molecular modeling calculation of $VCl_3(PMePh_2)_2$

The reaction of $VC1_3(THF)_3$ with $PMePh_2$ in toluene gave a red-purple solid of stoichiometry $VCl_3(PMePh_2)_2$. Single crystals suitable for X-ray structure determination were obtained by recrystallization from a pentane solution at low temperature. The structure of the complex was first published in the mid 80′s, [27][27a,c] and is here reported again, as obtained under different conditions (130 K instead of 113 K, [27][27a] and room temperature [27c]), owing to the significantly improved accuracy of the data. The structure of the two molecules (A and B) present in the asymmetric unit of $VCl_3(PMePh_2)_2$ is shown in Fig. 1. Both independent molecules adopt a conformation where the P—C_{methyl} bonds are not eclipsed but overlap with the P—C_{phenyl} bonds. An intriguing feature of the present structure was its distortion from a trigonal-bipyramidal geometry, as denoted by the deviation from 180° of the P—V—P angles, 171.71(2) and 166.34(2)° for A and B, respectively. Such distortion was noticed also in $VCl_3(IMes)_2$ (IMes = 1,3-dimesitylimidazol-2-ylidene) [34], having C—V—C angle equal to 164.84°, but not in $VCl_3(NMe_3)_2$ (N—V—N, 179.03°) [35], the only other trigonal-bipyramidal structures of V(III) present in the CSD [36], and it was found to be consistent with the observed lack of three-fold symmetry in the VCl_3 unit. In the distorted structures, in fact, one V—Cl bond length was found systematically shorter than the other two (V—Cl, 2.1855(8), 2.2535(7) and 2.2558(7) Å in molecule A; 2.1740(9), 2.2471(7) and 2.2563(7) Å in molecule B; 2.221, 2.266 and 2.268 Å in $[VCl_3(IMes)_2]$) [34]. The distortion out of the trigonal-bipyramidal geometry was alternately ascribed to forces bending the two large ligands off collinearity [27a], packing forces, and intramolecular steric effects [27c].

In order to ascertain the origins of such distortion, molecular modeling calculations have been performed on the isolated $VCl_3(PMePh_2)_2$ molecule by optimizing its geometry in gas-phase. While calculations accurately reproduced the X-ray V—P distances (2.535 Å vs. 2.528(7) on average for A and B), they provided an almost collinear geometry for the complex (P—V—P angle equal to 176°) and, accordingly, coincident V—Cl bond lengths, all measuring 2.242 Å, close to the experimental average value [2.229(8) Å]. Such disagreement can be imputed to the neglecting, in the present calculations, of the crystal environment, suggesting that packing forces, rather than intrinsic effects, are responsible for the molecular distortion of $VCl_3(PMePh_2)_2$ in solid state. Analysis of the intermolecular interactions network in the crystal structure revealed the presence of several C—H···Cl^- contacts [37] in the range 2.75–2.82 Å, well below the sum of the van der Waals of H and Cl, 2.95 Å [38]. Interestingly, optimization of the hypothetical 'eclipsed' structure of the complex, where P—C_{methyl} bonds overlap each other, leaded to a stable, almost collinear structure (P—V—P angle equal to 178°), isoenergetic with the observed one (with P—C_{methyl} bonds overlapping with P—C_{phenyl} bonds) within the accuracy of calculations, indicating that the adoption of the latter in solid state is as well ascribable to intermolecular interactions.

3.2. Catalytic behaviour

Series of ethylene polymerizations were performed with $VCl_3(PMePh_2)_2$ and, for comparison, with $VCl_3(THF)_3$ and VCl_3. Two different aluminum alkyls, i.e., Et_2AlCl and MAO, were used, both in the presence and absence of ETA. The results are summarized in Table 1.

Polymerizations with VCl_3 failed to produce poly(ethylene) (PE). Some activity was observed only in the presence of Et_2AlCl and ETA, but the yield remained extremely low (Table 1, entry 10). $VCl_3(PMePh_2)_2$ and $VCl_3(THF)_3$, in combination with Et_2AlCl, gave from low to good activities. Low activities were registered in the absence of reoxidant likely due to the rapid formation of inactive V(II) [13], while good activities were obtained in the presence of ETA (Table 1, entry 1 vs 2, and entry 5 vs 6), confirming that it plays a fundamental role in restoring the original trivalent oxidation state of vanadium [39]. By using MAO in place of Et_2AlCl only traces of PE were recovered without ETA (Table 1, entry 1 vs 3, and 5 vs 7) while a modest activity was observed in the co-presence of reoxidant (Table 1, entry 8).

This result can be likely due to the different nature of the ion pairing species formed by the two aluminum alkyls. Indeed, the cationic V–alkyl species formed by vanadium complexes and

Et_2AlCl was observed to be in an equilibrium between chloro-bridged and cationic alkyl species due to the smaller bulkiness and stronger nucleophilic nature of Et_2AlCl [12a], while an isolated cationic species would be formed in the presence of MAO. The equilibrium by Et_2AlCl would stabilize the V(III) species, leading to higher polymerization activities.

PEs obtained from $VCl_3(PMePh_2)_2$ were semicrystalline products with a melting temperature of 127 °C, a crystallinity of about 74% (ΔH_m = 220 J/g), a number of methyl branches in the order of 11–13 per 1000 carbon atoms, and molecular weights higher than those from $VCl_3(THF)_3$.

Preliminary studies of E/NB copolymerization with $VCl_3(PMePh_2)_2$, $VCl_3(THF)_3$ and VCl_3, in combination with Et_2AlCl, were performed in toluene at atmospheric pressure and room temperature. A series of experiments were carried out at different comonomers feedstock compositions (NB/E from 0.5 to 6). The results are summarized in Table 2.

None of the V(III) complexes was practically active in the homopolymerization of norbornene. On the contrary, when both ethylene and norbornene were available for the cationic vanadium active species, an extremely rapid copolymerization took place: $VCl_3(PMePh_2)_2$ and $VCl_3(THF)_3$ were instantaneously activated and the reaction was accompanied by a color shift to orange. The enhanced copolymerization activity may be likely due to the coordination of the highly nucleophilic and sterically encumbered norbornene cyclic olefin which is expected to stabilize the active species, and to reduce the electrophilicity of vanadium center [40]. As in the case of ethylene homopolymerization, moderate activities were registered in the absence of ETA, while excellent activities were attained with the reoxidant. It should be pointed out that $VCl_3(PMePh_2)_2$ gave activities comparable to those of $VCl_3(THF)_3$ despite a considerable difference in the ligand steric and electronic properties. Possibly, as generally accepted for phosphine-containing catalysts [41], $VCl_3(PMePh_2)_2$ is activated through a dissociative mechanism and the structure of vanadium active site is different from that in which we assume two phosphines around the metal. Indeed, both the labile $PMePh_2$ and THF ligands could be easily abstracted by the aluminum alkyl [42]. Nonetheless, what we can state with confidence, is that the ligand abstraction should be only partial and governed by equilibrium. This is because no activity was observed with VCl_3 (Table 2, entry 25), meaning that the presence of THF and $PMePh_2$ ligand in the coordination sphere of vanadium is necessary to the catalytic cycle.

Moreover, with the aim of validating the dissociative mechanism, we carried out the same copolymerization by VCl_3/Et_2AlCl/ETA but with the addition of free $PMePh_2$ (10 equiv to V). In this case, the polymerization productivity remained very low (Table 2, entry 26), confirming that $VCl_3(PMePh_2)_2$ should be activated through a dissociative mechanism where the dissociation of the phosphine is the first and possibly the rate-determining step.

Worth noting is that, as depicted in Fig. 2, the polymerization activity of $VCl_3(THF)_3/Et_2AlCl$/ETA was always slightly higher than that of $VCl_3(PMePh_2)_2/Et_2AlCl$/ETA. Such difference may be likely ascribed to different ratios of the dissociated ligand re-insertion rate to the (co)monomers insertion/coordination rate in the two cases. Indeed, the cationic V(III) species is not a particularly hard Lewis acid, and the replacement of the electronegative chlorides in $VCl_3(L)_n$ (L = generic ligand) by an ethyl group and the polymer growing chain increases the covalent character of the bonding in the complex. In this situation, re-addition of the dissociated hard THF Lewis base should be slower than successive insertions of the weaker Lewis base (co)monomers, while re-addition of phosphine should compete with coordination and insertion of (co)monomers [43]. This competition could play a key role in giving lower activities in the case of $VCl_3(PMePh_2)_2$. To support this thesis, we repeated the copolymerization experiment catalyzed by

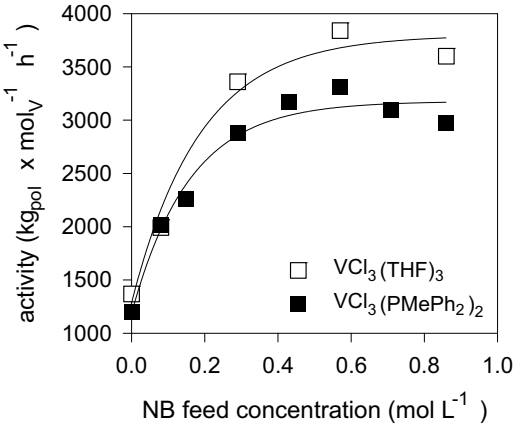

Fig. 2. Plot of catalytic activity vs norbornene feedstock concentration. The solid lines are guides to the eye and illustrate the overall trend.

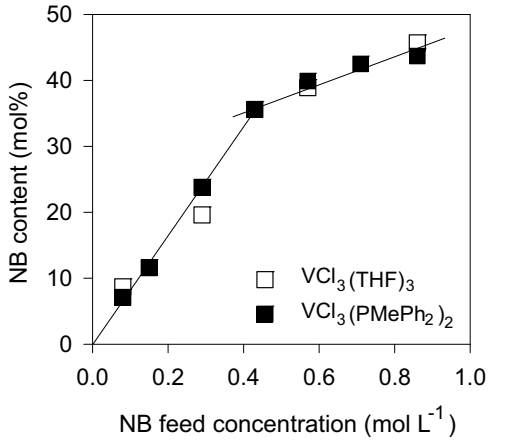

Fig. 3. Norbornene content in the copolymer vs norbornene feedstock concentration. The solid lines are guides to the eye and illustrate the overall trend.

$VCl_3(THF)_3/Et_2AlCl$/ETA (Table 2, entry 22) but with the addition of free $PMePh_2$ (10 equiv to V, Table 2 entry 24). By adding the phosphine, the activity decreased from 3840 to 3250 kg_{pol} mol_V^{-1} h^{-1}, thus confirming our claim and data reported with a cationic V(III) complex containing a cyclopentadienyl–amine ligand in the presence of PMe_3 [44].

Regarding the influence of norbornene feedstock concentration on the activities, it is shown in Fig. 2 that the activity increased with increasing NB/E ratio up to a plateau. There is a marked increasing dependence of the activity on norbornene concentration up to 0.43 mol/L likely due to a facile comonomer coordination [45], and to the fact that the copolymerization was preferred to the homopolymerization of each of the two monomers.

It seems that the incorporation of norbornene is somehow independent of the catalyst structure (Fig. 3). The comonomer content in the copolymers increased linearly with the norbornene feed concentration from 0.08 to 0.43 mol/L after which increased slightly up to 43.7 and 45.7 mol% for $VCl_3(PMePh_2)_2$ and $VCl_3(THF)_3$, respectively.

3.3. Molecular weight and chain-end analysis

All the copolymers possessed unimodal and relatively narrow molecular weight distribution (M_w/M_n = 1.6–3.5) consistent with the predominance of a single homogenous catalytic active species. Copolymers with high molecular weight were obtained in the absence of ETA, while in the presence of the reoxidant both the

Table 2
Copolymerization of ethylene with norbornene catalyzed by $VCl_3(PMePh_2)_2$, $VCl_3(THF)_3$, and VCl_3 in combination with Et_2AlCl and in the presence or absence of ETA and free $PMePh_2$.[a]

entry	NB (mol/L)	[NB]/[E][b]	yield (g)	activity[c]	NB[d] (mol%)	M_w[e] ($\times10^{-3}$)	M_w/M_n[e]	T_g (T_m)[f] (°C)
$VCl_3(PMePh_2)_2/Et_2AlCl$								
11	0.57	4	0.17	408	38.4	145.0	1.7	93
$VCl_3(PMePh_2)_2/Et_2AlCl/ETA$								
12	0.08	0.5	0.84	2016	7.1	17.1	3.5	0 (127)
13	0.15	1	0.94	2256	11.6			23 (126)
14	0.29	2	1.20	2880	23.8			42 (126)
15	0.43	3	1.32	3168	35.6	19.5	1.9	33
16	0.57	4	1.38	3312	39.9	19.2	2.1	60
17	0.71	5	1.29	3096	42.5	17.8	2.0	83
18	0.86	6	1.24	2976	43.7	17.6	2.2	86
$VCl_3(THF)_3/Et_2AlCl$								
19	0.57	4	0.33	792	37.8	103.5	1.8	77
$VCl_3(THF)_3/Et_2AlCl/ETA$								
20	0.08	0.5	0.83	1992	8.7	13.7	5.2	1 (122)
21	0.29	2	1.40	3360	19.6			41 (122)
22	0.57	4	1.60	3840	38.9	11.9	1.9	45
23	0.86	6	1.60	3840	45.7	9.0	2.1	42
$VCl_3(THF)_3/Et_2AlCl/ETA + PMePh_2$								
24	0.57	4	1.35	3250	39.2	20.2	1.9	46
$VCl_3/Et_2AlCl/ETA$								
25	0.57	4	inactive					
$VCl_3/Et_2AlCl/ETA + PMePh_2$								
26	0.57	4	traces					

[a] Polymerization conditions: ethylene pressure, 1.01 bar; total volume, 25 mL (toluene); V-complex, 5 μmol; Al/V = 2000; ETA/V = 300 temperature, 22 °C; time, 5 min.
[b] [NB]/[E] feed ratio (mol/mol) in liquid phase.
[c] Activity in $kg_{pol}\ mol_V^{-1}\ h^{-1}$.
[d] Determined by ^{13}C NMR.
[e] Determined by SEC. Determination of M_w of sample 13, 14 and 21 with a NB content from 11.6 to 23.8 mol% was complicated and the refractive index detection did not show a significant response.
[f] Determined by DSC.

V(III) complexes gave low–M_w polymers (Table 2, entry 11 vs 16, and entry 19 vs 22). Specifically, copolymers from $VCl_3(PMePh_2)_2$ had higher molecular weights than those obtained with $VCl_3(THF)_3$, and in some cases even double (Table 2). This result is somewhat analogous to that observed in the copolymerization of ethylene with 1-hexene catalyzed by mono(β-enaminoketonato)V(III) complexes and $VCl_3(THF)_3$. [19]. This result may be ascribed to the lower tendency of $VCl_3(PMePh_2)_2$ to give β–H elimination at a last enchained ethylene unit as revealed by the low amount of vinyl-end chain groups observed in the ^1H NMR spectra of copolymers. Indeed, formation of copolymers with low–M_w facilitated analysis of the chain-end structures by ^1H NMR, thus giving information about the reactions responsible for chain growth termination.

The ^1H NMR spectra of two representative copolymers obtained by $VCl_3(PMePh_2)_2$ (entry 16, NB = 39.9 mol%) and $VCl_3(THF)_3$ (entry 22, NB = 38.9 mol%) are shown in Fig. S1. The presence of various terminal and internal unsaturations, originating from a first event of β—H transfer to the metal or to the monomer [46], was registered. Three different multiplets were detected: (*i*) a quite broad signal in the range between 4.82 and 4.88 ppm, characteristic of vinyl chain end structures (V_E and V_{NB}, Chart S1), likely arising from a β–hydride elimination chain transfer from a last inserted ethylene unit, V–CH_2CH_2–P (P = polymer chain) [47], (*ii*) the multiplet centered at 5.13 ppm ascribed to internal vinylene end groups because of chain isomerization and allylic activation after ethylene insertion (I1–I5, Chart S2), and (*iii*) the multiplet centered at 5.31 ppm ascribed to unsaturated norbornenyl chain-start by C—H bond activation of a norbornene unit and further isomerization (NB-I, Chart S3) [46]. The ratio of internal/terminal double bond decreased from 3.5 to 2.5 for copolymers from $VCl_3(PMePh_2)_2$ and $VCl_3(THF)_3$, respectively. This means that $VCl_3(THF)_3$ is much prone to β—H transfer followed by a fast displacement of a vinyl-terminated copolymer, while for copolymerization by $VCl_3(PMePh_2)_2$, the initial event of β—H transfer is preferentially followed by successive β—H elimination, double bond rotation, reinsertion and isomerization.

3.4. Thermal properties

DSC heating profiles of all the copolymers obtained at very low norbornene feedstock concentration (Table 2, entries 12–14, and 20–21) showed both a glass transition event and a melting endotherm, likely due to a non-uniformity of the semi-batch copolymerization process, leading to a non-homogenous composition distribution. In these conditions, the copolymer chains are norbornene-rich at the beginning, and ethylene-rich at the end of polymerization. To ascertain that the obtained materials were not a mixture of PE and the copolymer, fractionation with boiling solvents were carried out, showing no PE or poly(norbornene) as a by-product. This means that the copolymerization is always preferred to the homopolymerization of either ethylene or norbornene.

On the other hand, by increasing the NB/E ratio (Table 2, entries 15–19 and 22–24), the copolymers showed only a single T_g, consistent with a completely amorphous structure. T_gs of the copolymers from $VCl_3(THF)_3$ (Table 2, entries 22–24) did not increase with increasing norbornene content, while T_gs of those from $VCl_3(PMePh_2)_2$ increased with it (Table 2, entries 15–19), as in general observed for poly(E-*co*-NB)s [5c] Moreover, T_gs for $VCl_3(THF)_3$ are always lower than those for $VCl_3(PMePh_2)_2$ at comparable norbornene incorporation. These facts indicate that copolymers from $VCl_3(THF)_3$ are less homogenous in terms of composition distribution also at higher norbornene feedstock loading.

In the light of these results, with the aim to perform the study of the catalytic mechanism involved in the copolymerization for the two V(III) complexes, we set new experiments at NB/E = 4 and reaction times in the order of seconds to ensure the uniformity of

Table 3
Microstructure analysis of E/NB copolymers by ^{13}C NMR.

entry	NB[a]	NB unit[b] (mol%)		
	(mol%)	isolated	alternated (iso:syndio)	dyads
11	38.4	34	63 (30:33)	3
15	35.6	44	53 (26:27)	3
16	39.9	34	63 (31:32)	3
17	42.5	31	67 (35:32)	2
18	43.7	21	75 (34:41)	5
19	37.8	37	59 (29:30)	3
22	38.9	35	62 (31:31)	4
23	45.7	17	74 (34:40)	9
24	39.2	40	58 (30:28)	2

[a] Determined by ^{13}C NMR.
[b] Calculated from ^{13}C NMR spectra in the C2/C3 region (42–54 ppm).

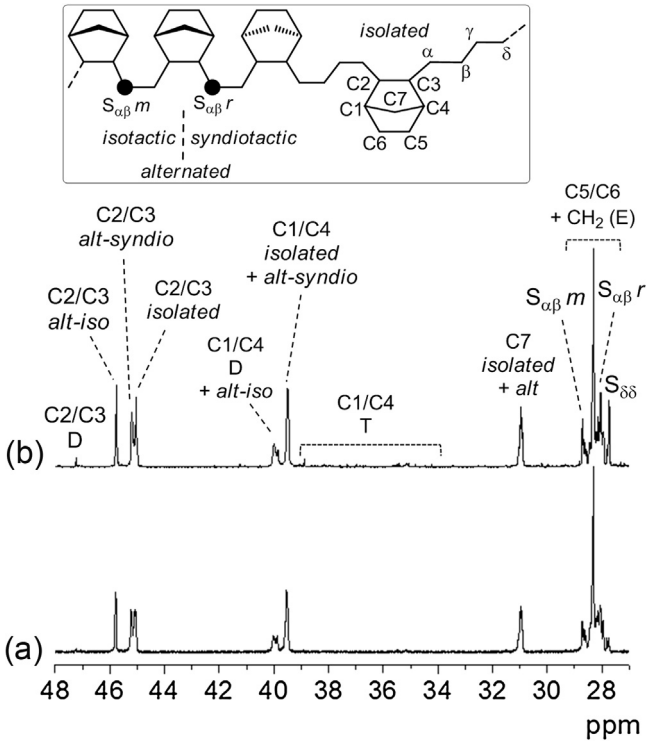

Fig. 4. ^{13}C NMR spectra of the E/NB copolymers obtained with (a) $VCl_3(PMePh_2)_2$ (entry 16, NB = 39.9 mol%) and (b) $VCl_3(THF)_3$ (entry 22, NB = 38.9 mol%).

the catalytic copolymerization process even in the presence of a relevant compositional drift (Table 4, entries 27 and 28).

3.5. Copolymers microstructure and catalytic mechanisms: determination of reactivity ratios

The microstructure of E/NB copolymers was investigated by ^{13}C NMR. The signals of each chemical shift region were assigned according to the literature, [4a,48] as follows: 42.0–54.0 ppm, C2/C3; 34.5–42.0 ppm, C1/C4; 31.0–34.5 ppm, C7; 26.0–31.0 ppm, C5/C6 and ethylene CH_2.

^{13}C NMR spectra of two copolymers obtained with $VCl_3(PMePh_2)_2$ (entry 16, NB = 39.9 mol%) and $VCl_3(THF)_3$ (entry 22, NB = 38.9 mol%) are shown in Fig. 4a and b, respectively. The spectra showed the typical pattern of alternating copolymers from an addition–type norbornene copolymerization with *cis exo-exo* enchainment. The dominant signals are those of alternating and isolated norbornene units, with traces of diads. The relative intensities of peak at 45.7 and 45.2 ppm, assigned to C2/C3 of NB in the alternating isotactic and syndiotactic NENEN sequences, respectively, also revealed that the copolymers have a random tacticity (Table 3).

Much work has been done to develop general procedures for the investigation of E/NB copolymers microstructure by ^{13}C NMR, [49–51] and hence to elucidate the copolymerization mechanism. The general methodology consists of two steps. Initially, the ^{13}C NMR spectrum is assigned [51], and the area under peculiar peaks related to known specific copolymer sequences is measured. Then, according to the stoichiometric relations developed in Ref. [49], binding these areas to the molar fractions of chain segments, a set of linear equations is built up to obtain suitable variables from which the complete tetrad molar fractions in the copolymer can be calculated by means of the equations given in Ref. [50]. This procedure allows to obtain a consistent description of the copolymer microstructure at the tetrad level. The linear system is overdetermined (i.e., it has more equations than unknowns) since certain variables can be equivalently defined by equations involving different peak areas from the spectrum. The solution of this linear system is typically carried out in the least squares sense (LS). The tetrad molar fractions obtained are considered as the experimental data to calculate the reactivity ratios, defining a first (MK1) or second (MK2) order Markovian copolymerization mechanism. In Ref. [50] equations are developed to calculate the tetrad molar fractions in a copolymer, given the reactivity ratios for a MK1 or MK2 mechanism, the comonomers feedstock ratio, and the norbornene incorporation. These equations assume a homogeneous Markov process for the copolymerization, where the conditional probabilities of insertion of the comonomers into the growing chain are constants. For this reason, they must be used under low conversion regimes ($\lesssim$5%), where the compositional drift taking place during the polymer formation, and consequent change in the insertion probabilities, can be neglected.

The second step consists in determining the reactivity ratios in order to minimize the discrepancy between the calculated and the experimental tetrad molar fractions. From the final agreement, and the values of the calculated reactivity ratios, a MK1 or MK2 mechanism is then attributed to the catalytic system under study. Again, the minimization procedure with respect to the reactivity ratios is carried out in the LS sense.

Direct application of these well-established protocols to the cases studied in this work was difficult for different reasons, affecting both the steps of the procedure. Concerning the first step, straightforward measurement of the peaks areas from the NMR spectrum was problematic and somewhat arbitrary, due to the extent of overlap among certain peaks of interest. Changes in the measured areas due to different definitions of the starting and ending points of the overlapping peaks, easily led to inconsistent results for the variables related to the tetrad molar fractions, especially the smallest ones. The sensitivity of the results of the overdetermined linear system to variations in the input areas was magnified by the

Table 4
Reactivity ratios calculated for first and second order markovian models.

entry	V-complex	activity[a]	NB[b] (mol%)	reactivity ratio calculation							
				r_1[c]	r_2[c]	*fit*[d] *MK1*	r_{11}[c]	r_{21}[c]	r_{12}[c]	r_{22}[c]	*fit*[d] *MK2*
27	$VCl_3(PMePh_2)_2$	17950	42.1	1.557	0.058	0.0058	1.605	1.550	0.058	0.073	0.0053
28	$VCl_3(THF)_3$	19340	43.2	1.424	0.062	0.0059	1.829	1.346	0.060	0.133	0.0037

Polymerization conditions: ethylene pressure, 1.01 bar; total volume, 25 mL (toluene); V-complex, 5 μmol; Et_2AlCl, Al/V = 2000; ETA/V = 300; temperature, 22 °C; time = 15 s; [NB]/[E] feed ratio (mol/mol) in liquid phase = 3.93.

[a] Activity in $kg_{pol}\ mol_V^{-1}\ h^{-1}$.

[b] Determined by ^{13}C NMR.

[c] The nomenclature for the reactivity ratios is the usual one where "1" relates to ethylene and "2" to norbornene. Definitions of these reactivity ratios in terms of the monomer insertion rate constants are given in Ref. [50].

[d] Mean absolute deviation between calculated and experimental tetrad fractions.

search of its solutions in the LS sense, which is known to be very sensitive to outliers in the data (in our context, some inaccurate peak area). In order to mitigate these problems, a deconvolution procedure of the NMR spectrum was previously set up to provide a more solid route in the evaluation of the peaks areas, and the linear system was solved in the more robust least absolute deviations (LAD), which is known to be much less sensitive to the outliers than LS, by means of the Barrodale-Roberts modified simplex method [52]. Concerning the deconvolution procedure, a homemade Fortran 90 parallel program was developed according to the OpenMP parallelization paradigm for shared memory computers, in order to implement a Richardson-Lucy deconvolution algorithm [29]. The method requires the NMR spectrum and the point-spread function (PSF) to be given in input. In our context the PSF is given as a single peak profile function. The algorithm builds up another spectrum by an iterative procedure, showing approximations to Dirac delta functions in the positions where peaks with the same profile given in input must be placed. The result of the calculation, then, reveals both the number and the positions of the peaks under the NMR spectrum, allowing for its representation in terms of a straightforward sum of scaled and shifted PSFs. Actually, the problem of deconvolution of the NMR spectrum is a *semi-blind* one, since we do not know everything about the true PSF. The result in terms of number and position of the constituent peaks, indeed, depends on the particular PSF we give in input. Anyway, the choice of the PSF is not completely arbitrary since some of its peculiar features are known: the theoretical peak of NMR spectra is a Lorentzian function, but field inhomogeneity and other experimental factors can give the peaks a partial Gaussian character. The so called pseudo-Voight profile (PV) is thus appropriate to model the peaks. This function is a linear combination of normalized Lorentzian and Gaussian curves, where the relative amount of each one is ruled by one weighting parameter. Beside this parameter, the half width at half maximum (HWHM) of the PV is to be decided. The initial choice of these parameters was performed as follows: the weighting function was set in such a way that the PV only contained contributions from the Lorentzian curve, and the HWHM was taken as the maximum value, allowing for a good decomposition of a certain portion of the NMR spectrum, chosen among those displaying peaks overlap. In this way, it was possible to describe the spectrum by the sum of the minimum possible number of PSFs. Determining the appropriate HWHM was a trial and error procedure involving different deconvolutions starting from large values of the HWHM and decreasing them until a good agreement between experimental and calculated profiles was obtained. Once plausible parameters for the PSF were determined, the deconvolution was applied to the whole spectrum, and finally the PV parameters, the height and the positions of the peaks were refined by a LS local minimization of the discrepancy between the calculated and experimental NMR spectra. This refinement was carried out by means of a subroutine distributed via web in [53], implementing a limited memory, bound-constrained quasi-Newton algorithm (L-BFGS-B) [54–56], after adaptation and inclusion in the homemade Fortran 90 deconvolution program. The proposed algorithm is very robust with respect to the presence of noise in the spectrum, so the deconvolution could be carried out without any preliminary smoothing of the data. The deconvolution of the whole spectra was thus obtained from the raw data (after correction for a linear baseline), and gave the decomposition of the profiles in terms of a minimum number of elementary peaks. An example of application of the described deconvolution process is shown in Fig. S3.

Concerning the calculation of reactivity ratios from the tetrad molar fractions, application of the equations given in Ref. [50] was not possible because both $VCl_3(PMePh_2)_2$ and $VCl_3(THF)_3$ complexes already produced comonomer conversions beyond 50% in experiments much less than one minute long, thus violating the fundamental requirement of those equations in order to be valid. An appropriate approach was than needed to calculate the reactivity ratios while keeping into account the high conversions in the experiments. Long-standing Skeist integral equation expresses the copolymer composition as a function of the conversion [57], and the Meyer-Lowry analytical integration provide a solution to it in closed form [58]. Other integral relations are reviewed in Ref. [28]. Anyway, use of the more detailed microstructure information at the tetrad level is best suited to allow a reliable assessment of a copolymerization mechanism and to accurately evaluate the related reactivity ratios. In order to solve the problem, an approach based on Monte Carlo simulation of the polymer chain growth, keeping into account the variation of the comonomer feed ratio during the reaction, was embedded into a suitable optimization procedure. The whole method, implemented in a homemade program in parallel OpenMP Fortran 90, consists in the optimization of the reactivity ratios for a chosen MK1 or MK2 mechanism, by means of a simulated annealing algorithm [59], so as to minimize the absolute deviation between the calculated and the experimental tetrad fractions. Robust minimization in the LAD sense is possible since the procedure does not require the calculation of derivatives of the function to be minimized with respect to the reactivity ratios. The evaluation of the deviation between calculated and experimental tetrads is obtained by explicitly generating a copolymer chain starting from a bath of labels representing the comonomers that reflects the feedstock composition. With assigned values of reactivity ratios and composition of feed, it is possible to determine the probability of monomers insertion given a certain chain termination [60]. The monomers are removed from the bath according to these probabilities and inserted at the end of the chain. After adding, the composition of the bath is updated and the termination of the chain is recorded: if the model is of the first order, the last monomer added is taken into account, otherwise, if the model is of second order, the last two terminals are considered. The new composition of the bath and the new chain-end determine new probabilities of comonomers insertion. The repetition of these steps until the degree of experimental conversion is reached, grows up a chain of labels that models a polymer where also the informa-

tion of the compositional variation and drift due to the norbornene conversion is contained. On this model chain, typically made by several millions monomers, the tetrad molar fractions are evaluated by a straightforward counting operation, and the absolute deviation between experimental and calculated data is evaluated. This chain growth procedure, giving the value of the absolute deviation between calculated and experimental tetrads as a function of the input reactivity ratios, is embedded into a simulated annealing procedure which repeatedly changes the reactivity ratios according to the specific criteria sketched below, and searches for those ones giving the minimum deviation.

The simulated annealing algorithm was chosen because of its conceptual simplicity and efficacy, and the fact that the number of parameters to be optimized is always quite limited (two or four reactivity ratios for MK1 or MK2, respectively), making more complex algorithms redundant for this type of problem [59]. Simulated annealing is a widely known and used global minimization algorithm, but it is worthwhile to spend some words about it, here. Concretely, such a cooling process is implemented as a Monte Carlo method where new values V_{new} of the reactivity ratios are proposed by changing their starting values V_{old} by a small (positive or negative) random amount. The starting values V_{old} correspond to a value F_{old} of the score function to be minimized, while the new ones correspond to a F_{new} value of this function. The proposed values V_{new} are then accepted or rejected according to the Metropolis-Hastings test [61,62], i.e., with a probability given by $min\{1,exp[(F_{old}\text{-}F_{new})/T]\}$, T being the "temperature" of the system. If the new parameters V_{new} are accepted, the further change will be performed on them, otherwise on V_{old} again. A sequence of change-acceptance-rejection of this type, started from some arbitrary values of the reactivity ratios produces an ensemble of values that compete to the temperature T. By slowly decreasing the temperature from a certain value of T_{max} to zero (in the program a linear cooling schedule is chosen), the desired effect of annealing is obtained, and at the end of the procedure, the values of the reactivity ratios yield the desired optimum. The program deals with both individual samples, and multiple sample sets. In the latter case, the score function is the sum of the individual samples score functions. Moreover, other quantities than the tetrads can be used, when available. Specifically, the program is able to manage microstructural information ranging from the bare content of comonomers up to the undecads in the copolymer, and copolymerization models beyond MK2.

The procedures described above were applied to the study of microstructure of two copolymers obtained from $VCl_3(PMePh_2)_2$ and $VCl_3(THF)_3$ (Table 4, entry 27 and 28, respectively). [NB]/[E] was set at 3.93 and the copolymerizations were quenched after 15 s to cope with the impressive activities (up to 19340 $kg_{pol}\ mol_V^{-1}\ h^{-1}$) of the two catalytic systems. However, despite the short polymerization time, the norbornene conversion was 53.3 and 54.3% for sample **27** and **28**, respectively. Once determined the tetrad molar fractions for the two samples, both MK1 and MK2 mechanisms were tested. Interestingly, while a first order mechanism satisfactorily described the microstructure of sample **27**, a second order one was shown to be more appropriate for sample **28**, indicating that $VCl_3(THF)_3$ may be more sensitive to the penultimate inserted monomer than $VCl_3(PMePh_2)_2$. The indications of possibly different copolymerization mechanisms for the two V(III) complexes are evident from calculations, as shown in Table 4. For sample **27**, passing from a MK1 to a MK2 model decreases the mean absolute deviation between the experimental and calculated tetrad fractions only to a negligible extent. Moreover, the reactivity ratios r_{11}, r_{21} from one side, and r_{12}, r_{22} from the other, are quite similar to each other and, in turn, quite similar to r_1 and r_2, respectively. These facts indicate that the catalytic mechanism is already captured by a MK1 process, and MK2 is redundant to

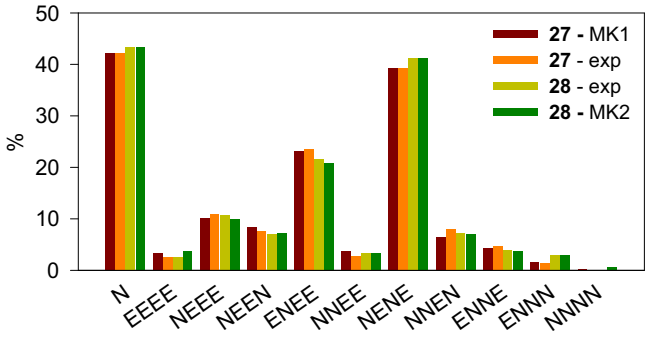

Fig. 5. Experimental and calculated tetrad distributions. Also the norbornene (N) content is shown.

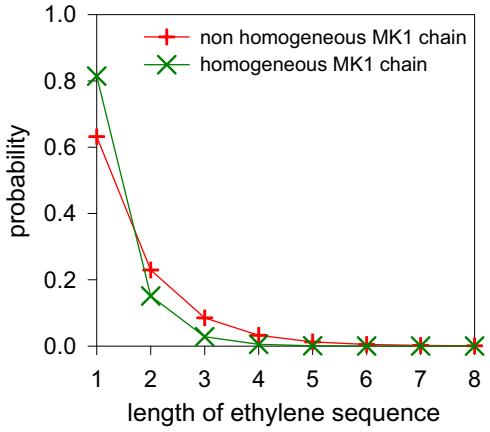

Fig. 6. Probability of ethylene sequences for entry **27** if the effects of the conversion are taken into account (non homogenous MK1 chain, red line) or neglected (homogenous MK1 chain, green line). (For interpretation of the references to colour in this figure legend, the reader is referred to the web version of this article.)

interpret the microstructure of the copolymer from $VCl_3(PMePh_2)_2$. On the contrary, for sample **28**, passing from MK1 to MK2 models more markedly reduces the disagreement between calculated and experimental microstructures, and the reactivity ratios r_{11}, r_{21} from one side, and r_{12}, r_{22} from the other, are more different from each other, and, in turn, different from r_1 and r_2, respectively. With respect to MK1, calculations with MK2 model improve the agreement between experimental and calculated NEEE, NEEN, ENNE, and ENNN tetrad molar fractions, leaving practically unaltered all the others. Anyway, it is clear from both the experimental data and calculations, that the microstructure at the tetrad level of the copolymers obtained in these specific experimental conditions by $VCl_3(PMePh_2)_2$ and $VCl_3(THF)_3$ are essentially the same, the differences between the two cases being quite small, as can be seen in Fig. 5. The more complex MK2 mechanism invoked for $VCl_3(THF)_3$ is required to fine tune the details of the microstructure, though the MK1 model already captured the main features of microstructure. The biggest microstructural differences between the copolymers generated by the two catalytic systems are about 2% for ENEE and NENE tetrads, and 1.5% for ENNN. The analysis presented above shows that the two copolymers are alternated ($r_1 r_2 \ll 1$). The most abundant tetrad is ENEN, followed by EENE with slightly more than one half of its frequency. The microstructures at tetrad level are essentially the same, even if $VCl_3(THF)_3$ complex seems to be more sensitive to penultimate effects than $VCl_3(PMePh_2)_2$.

In Fig. 6 the probability of the ethylene sequences in the copolymer is shown for the sample **27**, from which the average length of ethylene sequences can be calculated, being 1.60. In the plot it is also shown what the predicted probability should be if a homo-

Table 5
Copolymerization of ethylene with norbornene catalyzed by $VCl_3(PMePh_2)_2/Et_2AlCl/ETA$ at different ETA/V ratio.[a]

entry	ETA/V	yield (g)	activity[b]	NB[c] (mol%)	M_w[d] ($\times 10^{-3}$)	M_w/M_n[d]	T_g[e] (°C)
11[f]	–	0.17	408	38.4	145.0	1.7	93
29	10	1.30	3120	38.0	49.5	1.9	74
30	50	1.36	3264	36.8	38.3	1.9	65
31	150	1.50	3600	38.9	31.0	1.8	60
16[f]	300	1.38	3312	39.9	19.2	2.1	60
32	900	1.12	2688	40.9	10.1	1.8	24

[a] Polymerization conditions: ethylene pressure, 1.01 bar; total volume, 25 mL (toluene); $VCl_3(PMePh_2)_2$, 5 μmol; Al/V = 2000; [NB]/[E] = 4; temperature, 22 °C; time, 5 min.
[b] Activity in $kg_{pol}\ mol_V^{-1}\ h^{-1}$.
[c] Determined by ^{13}C NMR.
[d] Determined by SEC.
[e] Determined by DSC.
[f] First reported in Table 2.

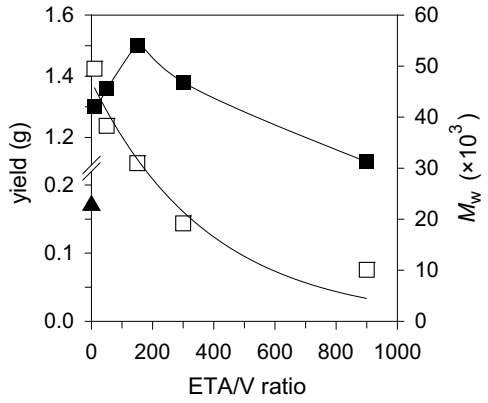

Fig. 7. Plot of copolymerization yield (■) and copolymers molecular weight (□) vs ETA/V mole ratio in the copolymerization by $VCl_3(PMePh_2)_2/Et_2AlCl/ETA$ at NB/E = 4 and 20 °C. Polymerization yield (▲) vs ETA/V ratio for the copolymer obtained with $VCl_3(PMePh_2)_2/Et_2AlCl$ at NB/E = 4 but without ETA is also shown (entry 11, M_w = 145,000 g/mol).

geneous MK1 chain with the reactivity ratios given in Table 4 is assumed for the catalytic mechanism, i.e., by neglecting the effects of the conversion. The impossibility to apply the standard assumption of a polymerization at low conversion regimes is manifest: finding the reactivity ratios under this assumption should have resulted in very wrong values for these quantities.

3.6. *Effect of copolymerization conditions on E/NB copolymerization by $VCl_3(PMePh_2)_2/Et_2AlCl/ETA$*

A series of copolymerizations were performed with $VCl_3(PMePh_2)_2/Et_2AlCl/ETA$ at different ETA/V ratio from 10 to 900, and norbornene feedstock concentration of 0.57 mol L^{-1} (NB/E = 4). Relevant data are summarized in Table 5. As shown in Fig. 7, there was an approximate linear dependence of the activity on ETA/V ratio up to 150. It is worth noting that an excellent activity was observed also in the presence of a low excess of ETA (10 equiv to V, entry 29), while at higher amount of ETA the productivity drop off rapidly, implying that excess chloro reagent suppresses the copolymerization and potentially competes with (co)monomer coordination/insertion likely through a chelation of the carbonyl oxygen to the vanadium center [63].

The molecular weight of the copolymers was lowered increasing ETA concentration, meaning that the reoxidant behaved also as chain termination/transfer agent. Addition of 4.53 mmol of ETA (ETA/V = 900) gave a copolymer with a molecular weight lowered to 10.1×10^3 g mol^{-1} (Fig. 7). The copolymers obtained at different ETA/V ratio have comparable norbornene content (37–41 mol%), while T_gs increased from 24 to 74 °C with increasing the copolymers molecular weight. (Fig. S4).

We also examined the effect of Et_2AlCl dosage at norbornene feedstock concentration of 0.57 mol L^{-1} (NB/E = 4) and ETA/V = 300 (Table 6). The copolymerizations were performed over the range of Al/V from 250 to 4000. A relatively low excess of Et_2AlCl (Al/V = 250) was sufficient for exhibiting activity as high as 1848 $kg_{pol}\ mol_V^{-1}\ h^{-1}$. Then the activity increased gradually reaching a maximum value of 3360 $kg_{pol}\ mol_V^{-1}\ h^{-1}$ when Al/V = 4000. By contrast, the copolymer's composition and microstructure as well as the molecular weight were almost unchanged over the increasing of the Al/V ratio, confirming that the chain transfer to the aluminum was not the dominant chain transfer. This result is quite different from that observed for the polymerization of ethylene by *N*,*N*-chelating iminopyrrolide V(III) complex [64], but it is comparable to that for the copolymerization of ethylene with 1-hexene with mono(β-enaminoketonato)V(III) complexes [19].

With the feed of 2000 equivalents of Et_2AlCl, a series of copolymerizations were carried out at different temperature from 0 to 70 °C (Table 7). The activity decreased at higher temperature likely due to the rapid deactivation even for a short polymerization time (5 min) and in the presence of an excess of the reoxidant (300 equiv to V). The norbornene content in the copolymers increased from 37.0 mol% at 0 °C to 44.9 mol% at 70 °C. The copolymer's molecular weight decreased with temperature likely due to an increase of chain transfer side reactions, while the molecular weight distribution remained relatively narrow, meaning that the copolymerization took place with uniform catalytically active species even at 70 °C. By increasing the polymerization temperature, the molecular weight decreased from 98.0 to 7.0×10^3 g mol^{-1} and, in the same manner, the T_g decreased from 80 to 51 °C (Fig. S5).

4. Conclusions

We synthesized and fully-characterized a vanadium(III) complex bearing a $PMePh_2$ ligand. The structure of $VCl_3(PMePh_2)_2$ has been determined as having a distorted trigonal-bipyramidal geometry on account of intermolecular interactions. Homo- and co-polymerization of ethylene with norbornene by $VCl_3(PMePh_2)_2$ and, for comparison, by $VCl_3(THF)_3$ and VCl_3, in combination with different aluminum alkyls, is reported. $VCl_3(PMePh_2)_2$ is likely activated through a dissociative mechanism where the dissociation of the labile phosphine ligand was the first and possibly the rate-determining step. Substitution of phosphine with THF affects: (*i*) the activity likely due to the different competition of the re-insertion rate of dissociated ligand compared to the insertion/coordination of (co)monomers, and (*ii*) the copolymers molecular weight, being higher for those obtained with $VCl_3(PMePh_2)_2$ because $VCl_3(THF)_3$ was more prone to β—H elimination followed by a fast displacement of a vinyl-

Table 6
Copolymerization of ethylene with norbornene catalyzed by $VCl_3(PMePh_2)_2/Et_2AlCl/ETA$ at different Al/V ratio.[a]

entry	Al/V	yield (g)	activity[b]	NB[c] (mol%)	M_w[d] ($\times 10^{-3}$)	M_w/M_n[d]
33	250	0.77	1848	37.7	18.4	2.0
34	500	0.98	2352	39.9	17.5	1.9
35	1000	1.35	3240	40.4	18.5	2.0
16[e]	2000	1.38	3312	39.9	19.2	2.1
36	4000	1.40	3360	42.0	16.7	1.8

[a] Polymerization conditions: ethylene pressure, 1.01 bar; total volume, 25 mL (toluene); $VCl_3(PMePh_2)_2$, 5 μmol; ETA/V = 300; [NB]/[E] = 4; temperature, 22 °C; time, 5 min.
[b] Activity in $kg_{pol}\ mol_V^{-1}\ h^{-1}$.
[c] Determined by ^{13}C NMR.
[d] Determined by SEC.
[e] First reported in Table 2.

Table 7
Copolymerization of ethylene with norbornene catalyzed by $VCl_3(PMePh_2)_2/Et_2AlCl/ETA$ at different temperature.[a]

entry	T (°C)	yield (g)	activity[b]	NB[c] (mol%)	M_w[d] ($\times 10^{-3}$)	M_w/M_n[d]	T_g[e] (°C)
37	0	1.40	3360	37.0	98.3	2.4	80
16[f]	22	1.38	3312	39.9	19.2	2.1	60
38	50	0.65	1548	42.7	10.8	2.0	56
39	70	0.31	732	44.9	7.0	2.1	51

[a] Polymerization conditions: ethylene pressure, 1.01 bar; total volume, 25 mL (toluene); $VCl_3(PMePh_2)_2$, 5 μmol; Al/V = 2000; ETA/V = 300; [NB]/[E] = 4; time, 5 min.
[b] Activity in $kg_{pol}\ mol_V^{-1}\ h^{-1}$.
[c] Determined by ^{13}C NMR.
[d] Determined by SEC.
[e] Determined by DSC.
[f] First reported in Table 2.

terminated polymer. Additionally, copolymers from $VCl_3(THF)_3$ showed greater non-uniformity in terms of composition distribution with respect to those from $VCl_3(PMePh_2)_2$, likely due to a more pronounced sensitivity to the effects of the compositional drift in the semi-batch polymerization process. This strongly affects the copolymer's thermal properties, the copolymers from $VCl_3(PMePh_2)_2$ exhibiting higher T_gs.

A study of copolymers microstructure at tetrad level has been performed and the catalytic mechanisms elucidated with data collected from *ad-hoc.* experiments, designed to ensure the uniformity of the catalytic copolymerization process even in the presence of a relevant (and unavoidable) compositional drift. We found that $VCl_3(THF)_3$ was more sensitive to penultimate effects from the growing polymer chain, while copolymerizations with $VCl_3(PMePh_2)_2$ were well described by first-order Markov statistics. Anyway, the two catalysts produced copolymers with essentially the same microstructure. Motivated by the features of ^{13}C NMR spectra of these copolymers, a deconvolution procedure based on the Richardson-Lucy algorithm [29], has been implemented to provide a more solid route to peaks areas evaluation. Moreover, the impossibility to obtain samples at low conversion, under the polymerization conditions investigated, required a Monte Carlo based computational approach to be developed to go beyond the standard homogeneous Markov chain model, and fully keep into account the effects of the conversion on the reactivity ratios. Both computational tools rely on very general principles, so that their use is not limited to V(III)-based catalysts, but any case of binary copolymerization can be successfully treated without modifications of the algorithms.

Finally, excellent activity, high norbornene incorporation and a strong tendency to give alternating copolymers is observed for $VCl_3(PMePh_2)_2$ when used in combination with Et_2AlCl and ETA. The reoxidant loading, and the reaction temperature play a key role, affecting the activity, and the copolymers molecular weight and thermal properties. A very high activity is demonstrated with $VCl_3(PMePh_2)_2/Et_2AlCl/ETA$ system in the presence of a low excess of Et_2AlCl (250 equiv to V) and ETA (10 equiv to V) that may be of interest for industrial applications.

Acknowledgements

Financial support from MIUR in the framework of PON 2007–2013 DIATEME is acknowledged. The authors are very grateful to M. Mauri, F. Greco for the acquisition of NMR spectra, and D. Piovani for SEC measurements.

Appendix A. Supplementary data

Supplementary data associated with this article can be found, in the online version, at http://dx.doi.org/10.1016/j.molcata.2016.09.002.

References

[1] (a) X. Li, Z. Hou, Coord. Chem. Rev. 252 (2008) 1842–1869;
(b) R.R. Lamonte, D. Mc Nally, Adv. Mater. Process. 159 (2001) 33–36;
(c) W. Kaminsky, Catal. Today 62 (2000) 23–34;
(d) W. Kaminsky, M. Arndt, Adv. Polym. Sci. 127 (1997) 143–187.
[2] (a) W. Kaminsky, A. Bark, M. Arndt, Macromol. Chem. Macromol. Symp. 47 (1991) 83–93;
(b) W. Kaminsky, R. Spiehl, Makromol. Chem. 190 (1989) 515–526.
[3] (a) X.-Y. Tang, Y.-X. Wang, B.-X. Li, J.-Y. Liu, Y.-S. Li, J. Polym. Sci. A: Polym. Chem. 51 (2013) 1585–1594;
(b) S.-R. Liu, B.-X. Li, J.-Y. Liu, Y.-S. Li, Polymer 51 (2010) 1921–1925;
(c) T. Hasan, T. Ikeda, T. Shiono, Macromolecules 37 (2004) 8503–8509;
(d) Y. Qian, J. Huang, M.D. Bala, B. Lian, H. Zhang, Chem. Rev. 103 (2003) 2633–2690;
(e) P. Altamura, A. Grassi, Macromolecules 34 (2001) 9197–9200.
[4] (a) G. Leone, M. Mauri, S. Losio, F. Bertini, G. Ricci, L. Porri, Polym. Chem. 5 (2014) 3412–3423;
(b) L.-P. He, J.-Y. Liu, Y.-G. Li, S.-R. Liu, Y.-S. Li, Macromolecules 42 (2009) 8566–8570;
(c) K. Vijayakrishna, G. Sundararajan, Polymer 47 (2006) 8289–8296;
(d) M. Gao, C. Wang, X. Sun, C. Qian, Z. Ma, S. Bu, Y. Tang, Z. Xie, Macromol. Rapid Commun. 28 (2007) 1511–1516;
(e) Y. Yoshida, S. Matsui, T. Fujita, J. Organomet. Chem. 690 (2005) 4382–4397.
[5] (a) M. Chen, W. Zou, Z. Cai, C. Chen, Polym. Chem. 6 (2015) 2669–2676;
(b) Y. Li, M. Gao, H. Gao, Q. Wu, Eur. Polym. J. 47 (2011) 1964–1969;
(c) G.M. Benedikt, E. Elce, B.L. Goodall, H.A. Kalamarides, L.H. McIntosh, L.F.

Rhodes, K.T. Selvy, C. Andes, K. Oyler, A. Sen, Macromolecules 35 (2002) 8978–8988.
[6] (a) Y. Chen, S. Mandal, A. Sen, Organometallics 29 (2010) 3160–3168; (b) K.M. Skupov, P.R. Marella, J.L. Hobbs, L.H. McIntosh, B.L. Goodall, J.P. Claverie, Macromolecules 39 (2006) 4279–4281; (c) Y.-C. Lin, K.-H. Yu, S.-L. Huang, Y.-H. Liu, Y. Wang, S.-T. Liu, J.-T. Chen, Dalton Trans. (2009) 9058–9067; (d) J. Kiesewetter, B. Arikan, W. Kaminsky, Polymer 47 (2006) 3302–3314.
[7] (a) B.L. Wang, T. Tang, Y. Li, D. Cui, Dalton Trans. (2009) 8963–8969; (b) Z. Hou, Y. Luo, X.J. Li, Organomet. Chem. 691 (2006) 3114–3121; (c) X. Li, J. Baldamus, Z. Hou, Angew. Chem. Int. 44 (2005) 962–965.
[8] D.L. Christman, G.I. Keim, Macromolecules 1 (1968) 358–363.
[9] (a) A. Zambelli, I. Pasquon, R. Signorini, G. Natta, Makromol. Chem. 112 (1968) 160–182; (b) E. Junghanns, O. Gumboldt, G. Bier, Makromol. Chem. 58 (1962) 18–42.
[10] (a) V.J. Murphy, H. Turner, Organometallics 16 (1997) 2495–2497; (b) Y. Doi, S. Suzuki, K. Soga, Macromolecules 19 (1986) 2896–2900.
[11] H. Kajiura, H. Oda, S. Minami, (Mitsui), EP 0 156 464 B1. http://www.mitsuichemicals.com/apel.htm, 1985.
[12] (a) K. Nomura, S. Zhang, Chem. Rev. 111 (2011) 2342–2362; (b) J.-Q. Wu, Y.-S. Li, Coord. Chem. Rev. 255 (2011) 2303–2314; (c) S. Gambarotta, Coord. Chem. Rev. 237 (2003) 229–243; (d) H. Hagen, J. Boersma, G. van Koten, Chem. Soc. Rev. 31 (2002) 357–364.
[13] K. Feghali, D.J. Harding, D. Reardon, S. Gambarotta, G. Yap, Q. Wang, Organometallics 21 (2002) 968–976.
[14] K.F. Hirsekorn, E.B. Hulley, P.T. Wolczanski, T.R. Cundari, J. Am. Chem. Soc. 130 (2008) 1183–1196.
[15] (a) W. Wang, K. Nomura, Adv. Synth. Catal. 348 (2006) 743–750; (b) W. Wang, K. Nomura, Macromolecules 38 (2005) 5905–5913.
[16] J.-B. Wang, L.-P. Lu, J.-Y. Liu, Y.-S. Li, Dalton Trans. 43 (2014) 12926–12934.
[17] J.-Q. Wu, J.-S. Mu, S.-W. Zhang, Y.S. Li, J. Polym. Sci. A: Polym. Chem. 48 (2010) 1122–1132.
[18] C. Lorber, F. Wolff, R. Choukroun, L. Vendier, Eur. J. Inorg. Chem. (2005) 2850–2859.
[19] L.-M. Tang, J.-Q. Wu, Y.-Q. Duan, L. Pan, Y.-G. Li, Y.-S. Li, J. Polym. Sci. A: Polym. Chem. 46 (2008) 2038–2048.
[20] J.-Q. Wu, L. Pan, Y.-G. Li, S.-R. Liu, Y.-S. Li, Organometallics 28 (2009) 1817–1825.
[21] J. Burt, W. Levason, G. Reid, Coord. Chem. Rev. 260 (2014) 65–115.
[22] M.L. Scheuermann, E.J. Johnson, P.J. Chirik, Org. Lett. 17 (2015) 2716–2719.
[23] T.J. Korstanje, J.I. van der Vlugt, C.J. Elsevier, B. de Bruin, Science 350 (2015) 298–302.
[24] C.H. Low, J.D. Nobbs, M. van Meurs, L.P. Stubbs, E. Drent, S. Aitipamula, M.H.L. Pung, Organometallics 34 (2015) 4281–4292.
[25] F. Bertini, I. Mellone, A. Ienco, M. Peruzzini, L. Gonsalvi, ACS Catal. 5 (2015) 1254–1265.
[26] G. Leone, A. Boglia, A.C. Boccia, S. Taglialatela Scafati, F. Bertini, G. Ricci, Macromolecules 42 (2009) 9231–9237.
[27] (a) R.L. Bansemer, J.C. Huffman, K.G. Caulton, Inorg. Chem. 24 (1985) 3003–3006; (b) D.G.L. Holt, L.F. Larkworthy, D.C. Povey, G.W. Smith, G.J. Leigh, Inorg. Chim. Acta 207 (1993) 11–19; (c) J. Bultitude, L.F. Larkworthy, D.C. Povey, G.W. Smith, J.R. Dilworth, J. Chem. Soc. Dalton Trans. (1986) 2253–2258; (d) J. Nieman, J.H. Teuben, J.C. Huffman, K.G. Caulton, J. Org. Chem. 255 (1983) 193–204.
[28] J.L. Koenig, Chemical Microstructure of Polymer Chains, John Wiley and Sons, New York, 1980.
[29] D.A. Fish, A.M. Brinicombe, E.R. Pike, J.G. Walker, J. Opt. Soc. Am. A 12 (1995) 58–65.
[30] Bruker, SMART, SAINT and SADABS; Bruker AXS Inc., Madison, Wisconsin, USA, 1997.
[31] G.M. Sheldrick, Acta Cryst. A 64 (2008) 112–122.
[32] G.M. Sheldrick, Acta Cryst. C 71 (2015) 3–8.
[33] M.J. Frisch, et al., Gaussian 09, Revision D.01, Gaussian, Inc., Wallingford, CT, USA, 2013.
[34] C. Lorber, L. Vendier, Dalton Trans. (2009) 6972–6984.
[35] P.T. Greene, P.L. Orioli, J. Chem. Soc. A. (1969) 1621–1624.
[36] F.H. Allen, Acta Cryst. B 58 (2002) 380–388.
[37] C.B. Aakeröy, T.A. Evans, K.R. Seddon, I. Pálinkó, New J. Chem. (1999) 145–152.
[38] A. Bondi, J. Phys. Chem. 68 (1964) 441–451.
[39] E. Addison, A. Deffieux, M. Fontanille, K. Bujadoux, J. Polym. Sci. A: Polym. Chem. 32 (1994) 1033–1047.
[40] Y. Yoshida, J.-I. Mohri, S.-I. Ishii, M. Mitani, J. Saito, S. Matsui, H. Makio, T. Nakano, H. Tanaka, M. Onda, Y. Yamamoto, A. Mizuno, T. Fujita, J. Am. Chem. Soc. 126 (2004) 12023–12032.
[41] (a) The phosphine dissociation in the activation process of phosphine-containing Grubbs-Hoveyda Ruthenium complexes is a well-accepted mechanism. For example, see: F. Nuñez-Zarur, X. Solans-Monfort, L. Rodríguez-Santiago, M. Sodupe, Organometallics 31 (2012) 4203–4215; (b) G.C. Vougioukalakis, R.H. Grubbs, Chem. Eur. J. 14 (2008) 7545–7556; (c) M.S. Sanford, J.A. Love, R.H. Grubbs, J. Am. Chem. Soc. 123 (2001) 6543–6554.
[42] Y. Ma, D. Reardon, S. Gambarotta, G. Yap, H. Zahalka, C. Lemay, Organometallics 18 (1999) 2773–2781.
[43] T.R. Younkin, E.F. Connor, J.I. Henderson, S.K. Freidrich, R.H. Grubbs, D.A. Bansleben, Science 287 (2000) 460–462.
[44] G.L. Liu, D.J. Beetstra, A. Meetsma, B. Hessen, Organometallics 23 (2004) 3914–3920.
[45] H. Lasarov, K. Mönkkönen, T. Pakkanen, Macromol. Chem. Phys. 199 (1998) 1939–1942.
[46] (a) R. Marconi, L. Boggioni, A. Ravasio, F. Di Colo, I. Tritto, U.M. Stehling, Macromolecules 44 (2011) 795–804; (b) N. Ni Bhriain, H.-H. Brintzinger, D. Ruchatz, G. Fink, Macromolecules 38 (2005) 2056–2063; (c) V. Busico, R. Cipullo, N. Friederichs, H. Linssen, A. Segre, V. Van Axel, G. Castelli, Macromolecules 38 (2005) 6988–6996.
[47] When norbornene is the last inserted unit, the β–H elimination is disfavored because a necessary condition for the β–H elimination is the planar conformation of the VkC(α)kH(β) bond, which cannot be formed due to the endo position of the β–H atom in a V–polynorbornyl intermediate.
[48] (a) G. Ricci, G. Leone, A. Rapallo, P. Biagini, G. Guglielmetti, L. Porri, Polymer 52 (2011) 5708–5715; (b) D. Ruchatz, G. Fink, Macromolecules 31 (1998) 4674–4680.
[49] I. Tritto, C. Marestin, L. Boggioni, L. Zetta, A. Provasoli, D.R. Ferro, Macromolecules 33 (2000) 8931–8944.
[50] I. Tritto, L. Boggioni, J.C. Jansen, K. Thorshaug, M.C. Sacchi, D.R. Ferro, Macromolecules 35 (2002) 616–623.
[51] I. Tritto, L. Boggioni, D.R. Ferro, Coord. Chem. Rev. 250 (2006) 212–241.
[52] I. Barrodale, F.D.K. Roberts, Commun. ACM 17 (1974) 319–320.
[53] http://users.iems.northwestern.edu/~nocedal/lbfgsb.html.
[54] R.H. Byrd, P. Lu, J. Nocedal, SIAM J. Sci. Comput. 16 (1995) 1190–1208.
[55] C. Zhu, R.H. Byrd, P. Lu, J. Nocedal, ACM Trans. Math. Softw. 23 (1997) 550–560.
[56] J.L. Morales, J. Nocedal, ACM Trans. Math. Softw. 38 (2011) 1–4.
[57] I. Skeist, J. Am. Chem. Soc. 68 (1946) 1781–1784.
[58] V.E. Meyer, G.G. Lowry, J. Polym. Sci. Pol. Chem. 3 (1965) 2843–2851.
[59] S. Kirkpatrick, C.D. Gelatt, M.P. Vecchi, Science 220 (1983) 621–630.
The simulated annealing algorithm mimics the physical process of cooling a system. At high temperature the system populates high-energy configurations. As the temperature is lowered, the system configurations change, until the system itself reaches a minimum of energy proper to the final low temperature. If we interpret the absolute deviation between calculated and experimental tetrads as energy, and the set of values of the reactivity ratios as system configuration, we realize that the application of the cooling of this system is exactly the desired minimization of the discrepancy between calculated and experimental tetrad fractions with respect to the reactivity ratios.
[60] A. Turner Jr., G. Goldfinger, J. Chem. Phys. 12 (1944) 205–209.
[61] N. Metropolis, A. Rosenbluth, M. Rosenbluth, A. Teller, E. Teller, J. Chem. Phys. 21 (1953) 1087–1092.
[62] W.K. Hastings, Biometrika 57 (1970) 97–109.
[63] M.P. Shaver, L.E.N. Allan, V.C. Gibson, Organometallics 26 (2007) 2252–2257.
[64] B.-C. Xu, T. Ju, J.-Q. Wu, N.-H. Hu, Y.-S. Li, Dalton Trans. (2009) 8854–8863.